The coexistence of ferroelectricity and ferromagnetism in Mn-doped $BaTiO_3$ thin films*

Ding Bin-Feng(丁斌峰)[a)b)†] and Zhou Sheng-Qiang(周生强)[b)]

[a)] *Department of Physics and Electronic Information, Langfang Teachers College, Langfang* 065000, *China*
[b)] *State Key Laboratory of Nuclear Physics and Technology, Peking University, Beijing* 100871, *China*

(Received 18 June 2011; revised manuscript received 16 August 2011)

5-at% Mn-doped and undoped $BaTiO_3$ thin films have been grown under different oxygen partial pressures by Pulsed Laser Deposition (PLD) on platinum-coated sapphire substrates. X-ray diffraction (XRD) measurements for all the thin films reveal a similar polycrystalline single-phase perovskite structure. Ferroelectricity is observed in the Mn-doped and undoped $BaTiO_3$ thin films grown under relatively high oxygen partial pressure. Ferromagnetic coupling of the Mn dopant ions, on the other hand, is only seen in Mn-doped $BaTiO_3$ thin films prepared under low oxygen partial pressure in a wide temperature range from 5 K to 300 K, and is attributed to the enhanced exchange coupling between Mn dopants and electrons at oxygen vacancies. Our results show that the leakage current is decreased with the doped Mn, but increases the dielectric loss and decreases the dielectric constant, and the ferroelectricity is impaired. To produce ferromagnetism, oxygen vacancies are necessary, which unfortunately increase the leakage current. This confirms that the mutual interplay between the ferroelectricity and ferromagnetism can be tuned by exchange coupling of the doped-Mn and oxygen vacancies in the $BaTiO_3$ thin films.

Keywords: ferroelectricity, ferromagnetism, platinum-coated

PACS: 77.80.–e, 75.50.Bb, 81.15.–z **DOI:** 10.1088/1674-1056/12/127701

CPB WITHDRAWN

1. Introduction

Much work has been carried out in the field of perovskite oxides due to their relatively simple structure and widespread applications in making devices such as sensors, transducers and memories. Among the perovskite oxides, $BaTiO_3$ has been one of the most intensively studied compounds for more than 60 years.[1–5] $BaTiO_3$, is a typical ABO_3 perovskite oxide whose structure can be described as a set of BO_6 octahedra arranged in a cubic pattern, with the Ba^{2+} ions located in the spaces between the octahedra and the Ti^{4+} ions occupying the centre of the octahedra.[6] In order to improve the electric properties of $BaTiO_3$, various dopants have been introduced into bulk or thin film $BaTiO_3$ to substitute for the Ba^{2+} or Ti^{4+}. Wu *et al.*[7] demonstrated that a proper concentration of Mn dopants in $BaTiO_3$-based ceramics can significantly increase the dielectric constant and decrease the dielectric loss, which was explained by the reaction: $Mn^{4+} + 2Ti^{3+} \rightarrow Mn^{2+} + 2Ti^{4+}$. Cole *et al.*[8] fabricated a 5-mol% Mg-doped $Ba_{1-x}Sr_xTiO_3$ multilayer structure and showed that Mg-doping reduces the dielectric loss of $Ba_{1-x}Sr_xTiO_3$ to 0.008 and yields a smoother surface compared to undoped $Ba_{1-x}Sr_xTiO_3$.

Meanwhile, an increasing interest has been devoted to the so-called multiferroic materials which possess more than one type of ferroic order (ferromagnetic/antiferromagnetic, ferroelectric, ferroelastic, and ferrotoroidic).[9–13] Unfortunately, very few room temperature multiferroic materials have been found up to now. $BiFeO_3$ is one of the most widely studied multiferroic materials due to its high Curie temperature (1083 K) and Néel temperature (643 K). However, the large leakage current hampers its practical application in devices, and its intrinsic magnetization is antiferromagnetic coupling.[14–17] Very recently, $BaTiO_3$ has been proven both theoretically and experimentally to be multiferroic by doping or synthesis at the nanoscale.[18–24] As a typical ferroelectric material, $BaTiO_3$ has many advantages as compared with $BiFeO_3$, such as low leakage current, low dielectric loss, high dielectric constant, and a more

*Project supported by the National Natural Science Foundation of China (Grant Nos. 10875004 and 11005005) and the National Basic Research Program of China (Grant No. 2010CB832904).

†Corresponding author. E-mail: ding_binfeng@126.com

© 2011 Chinese Physical Society and IOP Publishing Ltd

reproducible preparation process. Since the *ab initio* calculation performed by Nakayama *et al.*[18] demonstrated the possibility to induce ferromagnetism in $BaTiO_3$ by doping with transition metal ions, much work has been done by several groups. Lin *et al.*[20] prepared epitaxially Co-doped $BaTiO_3$ thin films on Nb-doped $SrTiO_3$ substrates by pulsed laser deposition and observed ferromagnetic (FM) behaviour at room temperature. The largest saturation magnetization of 187 emu/cm^3 was obtained by tuning the thickness of the Co-doped $BaTiO_3$ thin films. The origin of this ferromagnetism is still under discussion and needs more experimental investigation. Other researchers have reported on ferromagnetism in undoped $BaTiO_3$ ceramics and ascribed it solely to point defects such as oxygen vacancies.[24]

Although the doping in $BaTiO_3$ has been intensively investigated so far, most work either has focused on its electric or magnetic properties and did not consider their mutual interplay. In the present paper, 5-at% Mn-doped $BaTiO_3$ polycrystalline thin films grown on Pt/sapphire have been investigated with an emphasis on the variation of mutual interplay between dielectric, ferroelectric and magnetic properties with the Mn doping and deposition oxygen pressure.

2. Experiment

High-purity $BaTiO_3$ (4N) powder and a mixture of high purity $BaTiO_3$ (4N) and MnO_2 (5N) powders were pressed and finally sintered at 1300 °C for 12 hours to obtain the undoped and Mn-doped $BaTiO_3$ ceramic targets, respectively. The 100-nm thick Pt bottom electrodes were sputtered on c-sapphire substrates outside the PLD chamber. The Mn-doped $BaTiO_3$ (BTMO) and $BaTiO_3$ (BTO) thin films were grown by PLD using a KrF excimer laser ($\lambda = 248$ nm) with a fixed repetition rate of 2 Hz and a deposition temperature of 650 °C. To investigate the ambient-gas partial pressure dependence of the electric and magnetic properties of the BTO and BTMO thin films, an oxygen partial pressure of 10 mTorr or 100 mTorr (1 Torr=1.33322×10^2 Pa) was applied. In the following the four samples presented in this paper are labeled BTO-10, BTO-100, BTMO-10, and BTMO-100, respectively. After deposition, the films were *in-situ* post-annealed for 30 minutes at 650 °C and subsequently cooled down to room temperature at a cooling rate of 5 K/min under a constant oxygen partial pressure of 200 mbar (1 bar=10^5 Pa). The thickness of the thin films was determined by step profilometry and strongly dependent on the oxygen partial pressure and slightly on the Mn content. The PLD growth conditions and film thickness are summarized in Table 1.

Table 1. Sample identification and corresponding PLD growth conditions and film thickness in units of nm.

ID	Temperature/°C	Pressure/mTorr	Thickness/nm
BTO-10	650	10	281
BTMO-10	650	10	272
BTO-100	650	100	224
BTMO-100	650	100	219

The crystal structure of the films was analysed by means of X-ray diffraction (XRD) using a Bruker D8 system with CuKα radiation. For electric measurements circular Au top electrodes with a diameter of 0.2 mm were deposited by magnetron sputtering on top of the as-prepared BTO and BTMO thin films using a metal shadow mask to form a parallel-plate capacitor with BTO or BTMO as the dielectric medium. The resulting sample geometry is Au/BTO/Pt/sapphire and Au/BTMO/Pt/sapphire from top to bottom. The dielectric properties of the BTMO and BTO films were analysed by an impedance analyser (Agilent 4294A) in the frequency range from 100 Hz to 100 kHz under a driving voltage of 50 mV, the polarization-electric field loops of the films were observed using a sawyer-tower circuit[25] at 10 kHz. The magnetic properties of the films were investigated by a superconducting quantum interference device magnetometer (Quantum Design MPMS).

3. Results and discussion

Figure 1 shows the XRD θ–2θ patterns of the BTMO and BTO thin films grown on Pt/c-sapphire substrates. Only diffraction peaks corresponding to the perovskite structure are observed, indicating that

CPB WITHDRAWN

the prepared thin films have a single perovskite phase. The BTO-100 film is preferentially (111)-oriented [Fig. 1(a)], and the BTMO-100 film reveals a random orientation [Fig. 1(c)], while the BTO-10 film and BTMO-10 film are highly (001)-oriented [Figs. 1(b) and 1(d)]. Both the doping and the decreasing of deposition pressure have broadened the diffraction peaks significantly, indicating a deterioration of the thin film crystallinity. Although the BTMO films contain 5-at% Mn, only perovskite phases are detected in the BTMO-10 and BTMO-100 films [Figs. 1(c) and 1(d)].

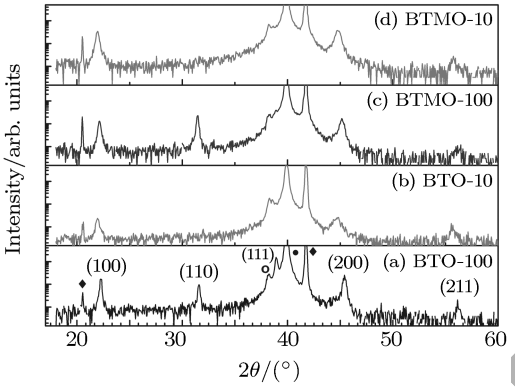


Fig. 1. XRD patterns of (a) BTO-100, (b) BTO-10, (c) BTMO-100, and (d) BTMO-10 thin films on Pt/sapphire substrates. XRD reflections labeled by the symbols ∘, ●, and ♦ represent Au, Pt, and *c*-sapphire, respectively.

In the following we discuss the influence of Mn doping on the electric and magnetic properties in $BaTiO_3$. The *I*–*IV* curves recorded on Au/BTO/Pt/*c*-sapphire and Au/BTMO/Pt/*c*-sapphire samples show basically symmetric characteristics, which can be attributed to the same barrier height of the interfaces between Au/perovskite and perovskite/Pt thin films, because of the similar work function of Au (5.10 eV) and Pt (5.65 eV), thus interface-limited conduction can be ruled out, or the variant potential barrier of the interfaces between Au/perovskite and perovskite/Pt thin films would result in the *I*–*IV* curves' larger asymmetric characteristics. Mn doping significantly decreases the leakage current by 1–2 orders of magnitude within different voltage ranges (Fig. 2(a)). For a better understanding of the conduction mechanism of the thin films, the *I*–*V* curves are presented on a double logarithmic scale [Fig. 2(b)]. It is interesting that the BTO-100, BTMO-10, and BTMO-100 thin films show different conduction behaviour. It has to be pointed out that the much higher leakage current of the BTO-10 thin film results from a shortening of all circular Au top contacts on this sample. The slope α of the $\log(I)$–$\log(V)$ curve for the BTO-100 thin film is constantly close to 2, implying that its leakage currents are dominated by space-charge-limited conduction (SCLC).[26] While the $\log(I)$–$\log(V)$ curve for the BTMO-10 and BTMO-100 thin films can be divided into two or three regions with different α of 2.8 and 8.4 for BTMO-10, 1.23, 1.84, and 6.13 for BTMO-100.

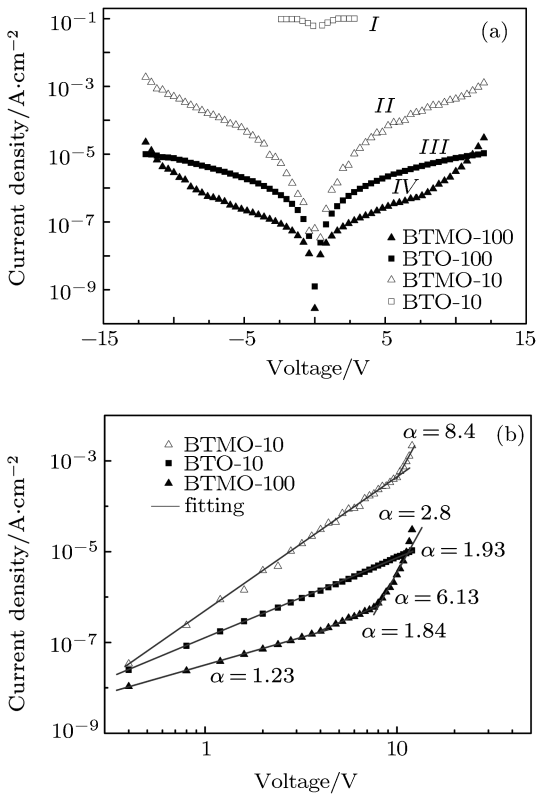


Fig. 2. Leakage current density of the BTO-100, BTMO-100, BTO-10, and BTMO-10 thin films.

According to Rose's SCLC theory,[27] the BTO-100 thin film with a constant $\alpha \approx 2$ can be simply explained using a model of a trap-free insulator or an insulator with shallow traps, both of which give a relation between the current and voltage as $I \propto V^2$. Meanwhile, the increase of α for the BTMO-10 and BTMO-100 thin films with increasing voltage involves one or two transition points which can also be interpreted by the SCLC mechanism.[27] It is well known that in perovskite oxides oxygen vacancies are abundant. The donor-like oxygen vacancies provide a large concentration of electrons in the conduction band acting as free carriers contributing to the leakage current. The Mn ions in $BaTiO_3$ have a fluctuating valence state between +2 and +4, which can compensate for the oxygen vacancies to keep the sample electrically neutral.[28] Mn dopant ions act as acceptors in the

CPB WITH

$BaTiO_3$ thin films and thus form positively charged trapping centres in the band gap. The trapping process can be described as follows:

$$\mathrm{Mn}_{\mathrm{Ti}}^{\times} + \mathrm{e}' = \mathrm{Mn}_{\mathrm{Ti}}', \quad (1)$$

$$\mathrm{Mn}_{\mathrm{Ti}}' + \mathrm{e}' = \mathrm{Mn}_{\mathrm{Ti}}''. \quad (2)$$

The generated electrons in the films are preferentially trapped at Mn atomic sites, because $\mathrm{Mn}_{\mathrm{Ti}}^{\times}$ and $\mathrm{Mn}_{\mathrm{Ti}}'$ are more reducible than $\mathrm{Ti}_{\mathrm{Ti}}^{\times}$.[29] In the low-voltage region, the Fermi level is fixed and the injected electrons from the electrode are trapped by the positive trapping centres formed by Mn ions as described by Eqs. (1) and (2). Only intrinsic carriers in the conduction band contribute to the current, resulting in an Ohmic conduction behaviour. As the voltage increases, the Fermi level is shifted towards the conduction band, part of the trapping states are occupied by the injected electrons, while the remaining trapping centres are at thermal equilibrium with electrons in the conduction band. This leads to the first change of α to the value of 2, indicating SCLC conduction. When the voltage further increases, the second sharp increase of α occurs at the so-called trap-filled limit voltage (V_{TFL}) given by the following equation[26]

$$V_{\mathrm{TFL}} = qN_{\mathrm{t}}d^2/2\varepsilon_r\varepsilon, \quad (3)$$

where N_{t} is the trap density, d is the film thickness, ε_r and ε represent the static dielectric constant of the thin film and free space, respectively. The values of V_{TFL} are 7.6 V and 10.4 V, and the static dielectric constants are measured to be 884 and 719 by the electrometer, for BTMO-100 and BTMO-10, respectively. Accordingly, their trap densities N_{t} are calculated to be 1.86×10^{19} cm^{-3} and 9.94×10^{18} cm^{-3}, respectively, which are 1–2 orders of magnitude higher than the results other groups reported for $BaTiO_3$-based systems.[30,31] The high trap density indicates an effective substitution of Ti ions by Mn ions and a reduced tendency of dopant cluster formation as compared with other reports.[30] Beyond the V_{TFL}, all trapping states are occupied and the electrons are directly injected into the conduction band, taking part in the conduction process and leading to a rapid increase of the current.[32] It should be noted that no Ohmic conduction behaviour can be observed in BTMO-10 and BTO-100, because the transition point from Ohmic conduction to SCLC conduction occurs at a very low voltage.

Based on the above discussion, the decrease of the leakage current in the BTMO-100 thin film is due to the formation of electron trapping centres caused by Mn acceptors in the band gap. Nevertheless, the BTMO-10 thin film shows leaky conduction even for high Mn doping concentration. This can be ascribed to the high concentration of free carriers offered by the large number of oxygen vacancies originating from the low oxygen pressure during growth.

Figure 3 shows the frequency dependence of the dielectric constant (ε_r) and the dielectric loss ($\tan\delta$) of the BTO and BTMO thin films. The $\tan\delta$ of the BTMO-10 thin film exhibits a noticeable drop within the low-frequency region, which indicates a large amount of trapping centres in the thin film. The $\tan\delta$ becomes nearly constant when the frequency increases above 10 kHz, because trapping centres are not able to respond to the high frequency. The reduction of the $\tan\delta$ of the BTMO-10 is consistent with the I–V curve, again proving a high density of oxygen vacancies in BTMO-10 due to the low oxygen pressure during the growth. On the other hand, it can be observed that the $\tan\delta$ of BTMO-100 and BTO-100 thin films do not show a large change over the whole frequency range, in addition, the BTMO-100 thin film displays higher $\tan\delta$ than the BTO-100 thin film at low frequency. Chu *et al.*[33] have reported that Mn-doping can reduce the $\tan\delta$ of BTMO thin films (the maximum concentration of Mn in their investigation was 1 at%). On the contrary, in our case the $\tan\delta$ of the BTMO-100 thin film is slightly higher than that grown under the same PLD growth condition. The higher $\tan\delta$ of the BTMO-100 thin film can be accounted for by the existence of trapping centres in the band gap as compared with the BTO-100 thin film, which agrees with the presence of three different regions in the I–V curve. At low frequency, those trapping centres cause the increase of $\tan\delta$.[28]

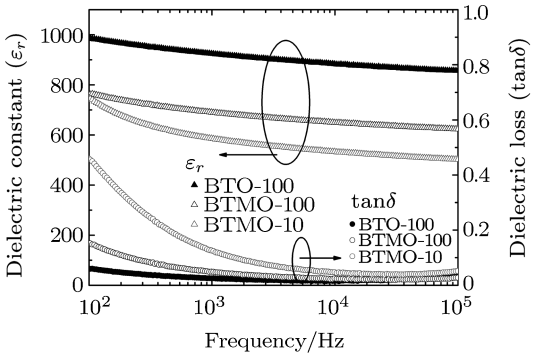


Fig. 3. Frequency dependence of the dielectric constant (ε_r) and dielectric loss ($\tan\delta$) of the BTO-100, BTMO-100, and BTMO-10 thin films.

CPB WITHDRAWN

The ε_r of the BTMO-100 and BTO-100 thin films is somewhat constant over the entire investigated frequency range. The ε_r of the BTMO-100 thin films is smaller than that of the BTO-100 thin films, indicating that an excessively high concentration of Mn-doping decreases the ε_r of BTMO thin films. This is consistent with the results of BTO ceramics reported by Wu *et al.*,[7] who ascribed their results to the dilution of the Ti by Mn. The ε_r of the BTMO-10 shows an obvious drop like the $\tan\delta$, also due to the space charges. Furthermore, the ε_r of the BTMO-10 is much lower than that of the BTMO-100 and BTO-100 thin films, implying a large number of defects in the sample. By using a measurement frequency of 10^4 Hz (Fig. 3), the ε_r and $\tan\delta$ of the BTMO-10, BTMO-100, and BTO-100 thin films are found to be 537, 654, 882, and 0.044, 0.023, 0.016 respectively.

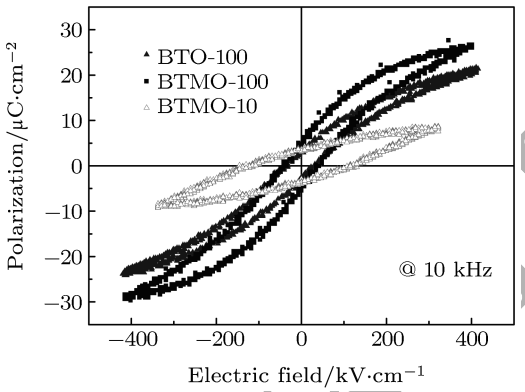


Fig. 4. Polarization-electric field hysteresis loops of the BTO-100, BTMO-100, and BTMO-10 thin films.

The P–E loops of the BTMO and BTO thin films measured by a sawyer-tower circuit at 10 kHz and an excitation AC signal of ±10 V are shown in Fig. 4. The P–E loops indicate a typical ferroelectric (FE) behaviour of the BTMO-100 and BTO-100 thin films. The remnant polarization P_r and coercive electric field E_c are $2P_r = 6.0$ μC/cm^2 and $2E_c = 64$ kV/cm for the BTMO-100 thin film and $2P_r = 9.6$ μC/cm^2 and $2E_c = 69$ kV/cm for the BTO-100 thin film. The $2P_r$ of the BTMO-100 thin film is larger than that of other reported pure polycrystalline BTO thin films grown on different substrates,[34–36] indicating a good crystalline quality of our sample. Even larger remnant polarizations are expected at higher electric fields for the BTMO-100 and BTO-100 thin films since the leakage current density (Fig. 2) at the highest electric field of 500 kV/cm for a given film thickness of 200 nm determined by the excitation AC signal of our instrument amounts to only 1.5×10^{-3} A/cm^2 and 1.64×10^{-3} A/cm^2, respectively. However, for the BTMO-10 thin film only a roundish PE curve has been obtained, in accordance with the large leakage current shown in Fig. 2, leading to the unsaturation of the PE curve.

The magnetization-field (M–H) hysteresis loops are shown in Fig. 5. The BTMO-10 shows an obvious ferromagnetic (FM) behaviour at room temperature, whereas the BTMO-100 exhibits paramagnetism only at low temperatures. In Ref. [22], the room-temperature ferromagnetism of the Mn-doped $BaTiO_3$ thin film was attributed to bound magnetic polarons[37] formed by localized electrons and Mn^{4+}, which has been widely used to explain the ferromagnetic behaviour in diluted magnetic semiconductors. While Xu *et al.*[21] observed ferromagnetism in Fe-doped $BaTiO_3$ ceramics and accounted for their results in terms of a model of carrier-mediated Zener-type Ruderman–Kittel–Kasuya–Yosida interaction,[38] Lee *et al.*[19] obtained ferromagnetic 5-at% Mn-implantated single crystalline $BaTiO_3$ at 10 K, but they were not able to determine whether the ferromagnetism was due to the bound magnetic polarons or the carrier-induced magnetism in the Zener-type mechanism. In particular, Tong *et al.*[23] synthesized non-stoichiometric Mn-doped $BaTiO_3$ nanoparticles with Ti-deficiency and observed ferromagnetism at low temperatures, and they explained it by means of a ferromagnetic exchange effect between holes trapped at Ti vacancies and magnetic Mn ions; their result agrees with the conclusion of Nakayama *et al.*[18] that hole-doped $Ba(Ti_{1-x}Mn_x)O_3$ should be ferromagnetic. Besides the transition metal ion-doped $BaTiO_3$ thin film and bulk materials, Mangalam *et al.*[24] reported room-temperature ferromagnetism in pure $BaTiO_3$ nanoparticles and ascribed it to oxygen vacancies which were identified by employing positron annihilation spectroscopy. The complexity of the different ferromagnetic coupling mechanisms of doped or virgin $BaTiO_3$ is therefore due to the various preparation processes.

In our case, a distinct difference in the M–H loops of BTMO-10 and BTMO-100 has been observed, revealing that the ferromagnetism strongly depends on the oxygen vacancy concentration in the samples which is caused by the different oxygen pressures during the PLD growth process. The observed ferromagnetism in BTMO-10, in contrast to the paramagnetism in BTMO-100, indicates that oxygen vacan-

CPB WITHDRAWN

cies are essential for introducing ferromagnetism into $BaTiO_3$ thin films. However, no ferromagnetism has been observed in pure $BaTiO_3$ (BTO-10) as shown in the inset of Fig. 5(a). This is believed to contain a comparable concentration of oxygen vacancies as BTMO-10, because BTO-10 and BTMO-10 were grown at the same oxygen pressure. Based on the above evidence, it is reasonable to conclude that both doping with Mn and the presence of oxygen vacancies play important roles in generating ferromagnetism in $BaTiO_3$. Lin *et al.*[20] reported significantly enhanced magnetism in their Co-doped $BaTiO_3$ as the thickness decreased, and attributed this to the possibility of more carriers being present in thinner films. However, they did not show the I–V curves of their samples. Our M–H curves along with the I–V curve clearly show that not only the doping with transition metal ions, but also the carrier density is a decisive factor to introduce room-temperature ferromagnetism in $BaTiO_3$ thin films.

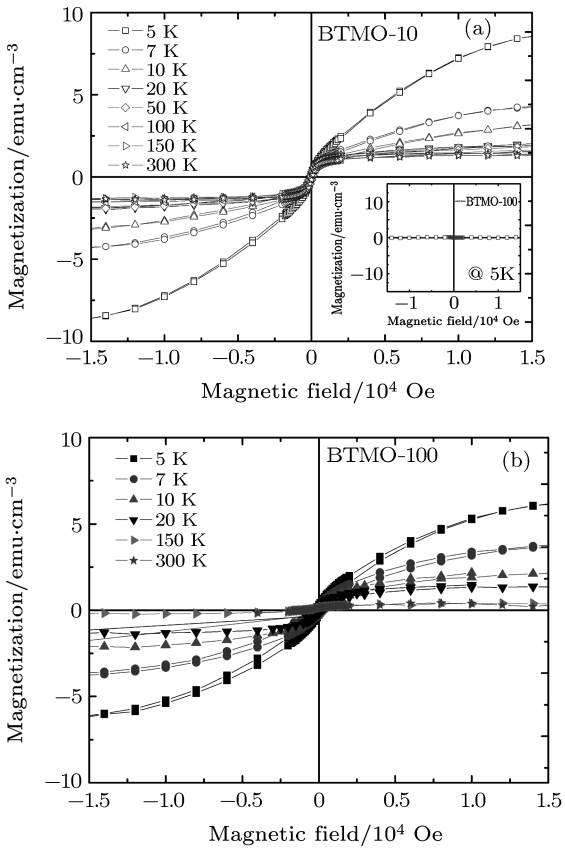


Fig. 5. Magnetization-field hysteresis loops of the BTMO-100 and BTMO-10. The inset of Fig. 5(a) shows M–H loop of BTO-10 at 5 K (1 Oe=79.5775 A/m).

Note that even for the BTMO-10 thin film with high oxygen vacancy concentration, not all Mn dopant ions are ferromagnetically coupled. The measured magnetic moment is attributed to isolated paramagnetic and ferromagnetically coupled Mn dopant ions which can be observed in Fig. 5(a). The paramagnetic component dramatically decreases with increasing temperature from 5 K and disappears at 150 K, while the ferromagnetic component is nearly temperature-independent, thus causing the observed room-temperature ferromagnetic behaviour.

Even though ferromagnetism has been obtained in BTMO-10, the small M_S value as compared with other typical ferromagnetic materials should be noticed, and its ferroelectricity deteriorated by the large leakage current caused by the oxygen vacancies. Ederer and Spaldin[39] have explained the difficulty realizing multiferroic perovskites[40,41] and they clarified the exclusivity between ferromagnetic and ferroelectric order in the $BaTiO_3$ system. To stabilize the off-centring of Ti ions which is essential for ferroelectricity, an energy-lowering covalent bond has to be formed, which requires empty d orbitals of the transition metal ions. However, the substitution of Ti ions by Mn ions destroys the stabilization of the off-centring displacement, which weakens the polarization as shown in the PE loops (BTMO-100). On the other hand, a partially occupied d shell of transition metal ions is needed for magnetization. Moreover, the ferromagnetic coupling[42] between Mn ions happens when a high concentration of oxygen vacancies is present, which increases the leakage current and thus further deteriorates PE (BTMO-10).

4. Conclusions

In conclusion, polycrystalline 5-at% Mn-doped $BaTiO_3$ and pure $BaTiO_3$ thin films were prepared on Pt/sapphire substrates at 100 mTorr and 10 mTorr oxygen pressures by pulsed laser deposition. The electric properties depend strongly on the oxygen vacancy concentration which is controlled by the deposition pressure and are also significantly influenced by doping with Mn. The leakage current is decreased by the substitution of Ti by Mn ions which form trapping centres in the $BaTiO_3$ band gap. The dielectric constant decreases and dielectric loss increases as compared with the pure $BaTiO_3$ thin film. The Mn-doped $BaTiO_3$ films with a large amount of oxygen vacancies show room-temperature ferromagnetic behaviour. On the contrary, neither the Mn-doped $BaTiO_3$ thin film with low oxygen vacancy concentration nor the

HDRAWN

pure $BaTiO_3$ thin film with high oxygen vacancy concentration exhibit ferromagnetism. The present work shows the dependence of the electric and magnetic properties on the Mn-doping and oxygen vacancy of the $BaTiO_3$ thin films; although doping with Mn can decrease the leakage current, which is very important for device application, the ferroelectricity is impaired. Besides, sole Mn doping is not enough for introducing room-temperature ferromagnetism, since oxygen vacancies are also necessary, but unfortunately they increase the leakage current. Therefore, the ferroelectricity and ferromagnetism can be tuned mutually by doped-Mn and undoped $BaTiO_3$ thin films grown under relatively high and low oxygen partial pressures, so that they are also coupling each other mutually in Mn-doped $BaTiO_3$.

References

[1] Vijatovic M M, Bobic J D and Stojanovic B D 2008 *Sci. Sintering* **40** 155

[2] Cheng H F, Yeh M H, Liu K S and Lin I N 1993 *Jpn. J. Appl. Phys.* **32** 5656

[3] Baniecki J D, Shioga T, Kurihara K and Kamehara N 2005 *J. Appl. Phys.* **97** 114101

[4] Yanase N, Abe K, Fukushima N and Kawakubo T 1999 *Jpn. J. Appl. Phys.* **38** 5305

[5] Choi K J, Biegalski M, Li Y L, Sharan A, Schubert J, Uecker R, Reiche P, Chen Y B, Pan X Q, Gopalan V, Chen L Q, Schlom D G and Eom C B 2004 *Science* **306** 1005

[6] Izyumskaya N, Alivov Y, Cho S J and Rev C 2007 *Solid State Mater. Sci.* **32** 111

[7] Wu S, Wang S, Chen L, Wang X and Mater J 2008 *Sci. Mater. Electron* **19** 505

[8] Cole M W, Ngo E, Hirsch S, Okatan M and P S 2008 *Appl. Phys. Lett.* **92** 072906

[9] Wang J, Neaton J B, Zheng H, Nagarajan V, Ogale S B, Liu B, Viehland D, Vaithyanathan V, Schlom D G, Waghmare U V, Spaldin N A, Rabe K M, Wuttig M and Ramesh R 2003 *Science* **299** 1719

[10] Kimura T, Goto T, Shintani H, Lshizaka K, Arima T and Tokura Y 2003 *Nature* **426** 55

[11] Hur N, Park S, Sharma P A, Ahn J S, Guha S and Cheong S W 2004 *Nature* **429** 392

[12] Duan C G, Jaswal S S and Tsymbal E Y 2006 *Phys. Rev. Lett.* **97** 047201

[13] Eerenstein W, Mathur N D and Scott J F 2006 *Nature* **442** 759

[14] Ederer C and Spaldin N A 2005 *Phys. Rev.* B **71** 060401

[15] Béa H, Bibes M, Barthélémy A, Bouzehouane K, Jacquet E, Khodan A, Contour J P, Fusil S, Wyczisk F, Forget A, Lebeugle D, Colson D and Viret M 2005 *Appl. Phys. Lett.* **87** 072508

[16] Sosnowska I, Neumaier T P and Steichele E 1982 *J. Phys.* C: *Solid State Phys.* **15** 4835

[17] Bai F, Wang J L, Wuttig M, Li J F, Wang N G, Pyatakov A P, Zvezdin A K, Cross L E and Viehland D 2005 *Appl. Phys. Lett.* **86** 032511

[18] Nakayama H and Yoshida H K 2001 *Jpn. J. Appl. Phys.* **40** L1355

[19] Lee J S, Khim Z G, Park Y D, Norton D P, Theodoropoulou N A, Hebard A F, Budai F J, Boatner L A, Pearton S J and Wilson R G 2003 *Solid-State Electron* **47** 2225

[20] Lin Y H, Zhang S, Deng C, Zhang Y, Wang X and Nan C W 2008 *Appl. Phys. Lett.* **92** 112501

[21] Xu B, Yin K B, Lin J, Xia Y D, Wan X G, Yin J, Bai X J, Du J and Liu Z G 2009 *Phys. Rev.* B **79** 134109

[22] Lin Y H, Yuan J, Zhang S, Zhang Y, Liu J, Wang Y and Nan C W 2009 *Appl. Phys. Lett.* **95** 033105

[23] Tong X, Lin Y H, Zhang S, Wang Y and Nan C W 2008 *Appl. Phys. Lett.* **104** 066108

[24] Mangalam R V K, Chakrabrati M, Sanyal D, Chakrabati A and Sundaresan A 2009 *J. Phys.: Condens. Matter* **21** 445902

[25] Sawyer C B and Tower C H 1930 *Phys. Rev.* **35** 269

[26] Lampert M A 1956 *Phys. Rev.* **103** 1648

[27] Rose T L, Lelliher E M, Scoville A N and Stone S E 1984 *J. Appl. Phys.* **55** 3706

[28] Takezawa Y, Kobayashi K, Nakasone F, Suzuki T, Mizuno Y and Imai H 2009 *Jpn. J. Appl. Phys.* **48** 111408

[29] Eichel R A 2007 *J. Electroceram.* **19** 9

[30] Wang S Y, Cheng B L, Wang C S, Dai S Y, Lu H B, Zhou Y L, Chen Z H and Yang G Z 2004 *Appl. Phys. Lett.* **84** 4116

[31] Tao K, Hao Z, Xu B, Chen B, Miao J, Yang H and Zhao B R 2003 *J. Appl. Phys.* **94** 4042

[32] Qi Y, Lu C, Zhang Q, Wang L, Chen F, Cheng C and Liu B 2008 *J. Phys.* D: *Appl. Phys.* **41** 065407

[33] Chu J P, Mahalingam T, Liu C F and Wang S F 2007 *J. Mater. Sci.* **42** 346

[34] Thomas R, Varadan V K, Komarneni S and Dube D C 2001 *J. Appl. Phys.* **90** 1480

[35] Huang L M, Chen Z Y, Wilson J D, Banerjee S, Robinson R D, Herman I P, Laibowitz R and O'Brien S 2006 *J. Appl. Phys.* **100** 034316

[36] Qiao L and Bi X 2009 *J. Eur. Ceram. Soc.* **29** 1995

[37] Coey J M D, Venkatesan M and Fitzgerald C B 2005 *Nat. Mater.* **4** 173

[38] Dietl T, Ohno H, Matsukura F, Cibert J and Ferrand D 2000 *Science* **287** 1019

[39] Ederer C and Spaldin N A 2004 *Nat. Mater.* **3** 849

[40] Li J J, Yu J, Li J, Wang M, Li Y B, Wu Y Y, Gao J X and Wang Y B 2010 *Acta Phys. Sin.* **59** 1302 (in Chinese)

[41] Guo D Y, Li C, Wang C B, Shen Q, Zhang L M, Tu R and Goto T 2010 *Acta Phys. Sin.* **59** 5772 (in Chinese)

[42] Zhao Q X, Ma J K, Geng B, Wei D Y, Guan L and Liu B T 2010 *Acta Phys. Sin.* **59** 8042 (in Chinese)

CPB WITHDRAWN